PHILOSOPHICAL TRANSACTIONS OF THE ROYAL SOCIETY A MATHEMATICAL, PHYSICAL & ENGINEERING SCIENCES

The Six Roll Mill: Unfolding an Unstable Persistently Extensional Flow

M. V. Berry and M. R. Mackley

Phil. Trans. R. Soc. Lond. A 1977 **287**, 1-16
doi: 10.1098/rsta.1977.0137

THE SIX ROLL MILL: UNFOLDING AN UNSTABLE PERSISTENTLY EXTENSIONAL FLOW†

By M. V. BERRY and M. R. MACKLEY‡
H. H. Wills Physics Laboratory, Tyndall Avenue, Bristol, BS8 1TL

(*Communicated by A. Keller, F.R.S. – Received 29 September* 1976)

[Plates 1–5]

The six roll mill produces steady two-dimensional flows with three incoming and three outgoing streams of fluid. Each flow is generated by a particular set of roller speeds represented by a point in 'control space', and is characterized by its 'critical points', at which the fluid velocity vanishes. A surface Σ separates control space into regions whose flows have different numbers of critical points; on Σ the critical points are degenerate. For the system studied, Σ is the 'elliptic umbilic catastrophe' in the classification of Thom. By using glycerol in the mill, a sequence of flows was explored, corresponding in control space to a loop intersecting Σ. The observed streamline patterns agree well with computer simulations.

When the mill contained a 2 % solution of polyethylene oxide in water the sequence of observed flow patterns was very different. This can be explained by the long chain molecules becoming persistently extended along the outgoing streamlines issuing from critical points, and the resulting sheets of high extension inhibiting the development of large strain rates in the outgoing fluid streams; the breaking of symmetry between inflows and outflows is shown to explain the observed flow patterns. The high extension of the polymer molecules was observed as intense localized flow birefringence. The diminution in this intensity near degenerate critical points can be used to give rapid estimates of macromolecular relaxation time.

1. Introduction

Infinitesimal lines of fluid particles issuing from any point in a flowing fluid are generally altering in length and rotating as well as translating. Flows where some such fluid lines continually increase in length are called 'persistently extensional'. Their importance in the context of this paper lies in their ability to stretch to substantially full extension initially tangled long-chain polymer molecules dissolved in the fluid, provided both the relaxation time of the chains and the rate of extension of fluid lines are sufficiently large.

For steady flows the recent work of Crowley, Frank, Mackley & Stephenson (1976) and Frank & Mackley (1976) shows that persistent extension occurs along streamlines issuing from stagnation points of the flow field; these are points where the fluid velocity vanishes (relative to rigid boundaries of the system, or to distant fluid). Frank & Mackley (1976) study two-dimensional flows with constant principal strain rate S and vorticity ω. They show that these stagnation points exist when the flow is strain rate dominated, i.e. when $S > \omega$, as *hyperbolic critical points* of the flow field, where two incoming and two outgoing streamlines meet. When the flow is vorticity dominated, i.e. when $S < \omega$, the fluid velocity vanishes at *elliptic critical*

† Dedicated to F. C. Frank, F.R.S., on his retirement as Director of the H. H. Wills Physics Laboratory.
‡ Now at School of Engineering and Applied Sciences, University of Sussex, Falmer, Brighton, Sussex.

points; these are surrounded by closed streamlines and are not sources of persistently extensional flow. Henceforth any place where the fluid velocity vanishes will be called a critical point.

The purpose of this paper is to examine in detail a family of two-dimensional persistently extensional flows associated with *degenerate critical points* at which $S = \omega$ where the fluid velocity vanishes. Such points are singularities of the flow; they have been classified by Thom (1972) and the classification forms the basis of 'catastrophe theory'. A degenerate critical point is unstable in that a generic perturbation of the flow field causes its associated streamlines to change topology and the critical point to break up into non-degenerate hyperbolic or elliptic critical points, or degenerate critical points whose degree of singularity is lower. This breaking-up can occur in a number of topologically different ways which can be completely enumerated for the simpler types of degenerate critical points (a proof is given by Arnol'd 1973). The family of topologically distinct flows into which a singular flow (that is a flow containing a singularity) can break up is called the 'universal unfolding' of the singular flow, and the changes of topology are the 'catastrophes'.

In the most singular flow considered here, three streamlines enter the singularity and three issue from it. The flow can be realized in the 'six roll mill', which consists of six alternately counter rotating rollers immersed in the fluid so that the parallel axes of the rollers form the edges of a regular hexagonal prism. The universal unfolding is the *elliptic umbilic* catastrophe of Thom's classification, and all the different flow patterns in this family can be produced by altering the controls of the rollers so that they may no longer all rotate at the same rate.

In the context of polymer chain extension there are two reasons for studying singular flows. The first is connected with the fact that at degenerate critical points, in contrast with hyperbolic critical points, fluid lines are not extending: the rate of persistent extension increases from zero along the streamline issuing from the singularity. This means that high extension of dissolved polymer molecules occurs not at the singularity but some distance from it. The region surrounding the singularity, containing chains that are not highly extended, can be observed as a 'hole' in the distribution of flow-induced birefringence. The size of this hole gives information about the relaxation time of polymer chains.

The second reason is connected with the fact that polymer chains are not passive indicators whose extension merely reveals localized birefringence issuing from stagnation points. In fact localized regions of high extension can modify the ambient flow (Frank & Mackley 1976) probably by inhibiting the development of high strain rates. With singular flows this effect can be dramatic: in the six roll mill a given sequence of roller control settings can produce a sequence of flows (within the elliptic umbilic family) that is very different in fluids with and without dissolved polymer.

2. Six roll mill flow field

In the two-dimensional flows under consideration the fluid velocity $\boldsymbol{u}$ has no component u_z, the components u_x and u_y do not vary with z, and the fluid is incompressible. Such flows can be represented by a stream function $\phi(\boldsymbol{R})$, where $\boldsymbol{R} = (x, y)$, as

$$\boldsymbol{u}(\boldsymbol{R}) = \nabla_\perp(\phi(\boldsymbol{R})\,\hat{\boldsymbol{z}}) = (\phi_y, -\phi_x, 0), \tag{2.1}$$

where $\hat{\boldsymbol{z}}$ is the unit vector in the z direction and subscripts on ϕ denote differentiation. It is helpful to think of ϕ as a curved surface whose infinitesimal deviation from the $\boldsymbol{R}$ plane is equal to $\phi(\boldsymbol{R})$. From (2.1) the streamlines are the contours of ϕ and the fluid speed is

$$|\boldsymbol{u}| = |\nabla\phi|. \tag{2.2}$$

Hyperbolic critical points are cols (saddle points) of the surface ϕ, and elliptic critical points are maxima or minima of ϕ.

Let C_1 and C_2 be the principal curvatures of ϕ at $\boldsymbol{R}$, reckoned positive if ϕ is concave towards $\phi = +\infty$, and let $C_1 \geqslant C_2$. Then the following results can be proved:

The *vorticity* is
$$\omega(\boldsymbol{R}) \equiv \tfrac{1}{2}\nabla_{\Lambda}\boldsymbol{u} = \omega\hat{\boldsymbol{z}}, \tag{2.3}$$

where
$$\omega(\boldsymbol{R}) = -\tfrac{1}{2}\nabla^2\phi = -(C_1+C_2)/2. \tag{2.4}$$

The *strain rate tensor* is
$$S_{ij}(\boldsymbol{R}) \equiv \begin{bmatrix} S_{xx} & S_{xy} \\ S_{yx} & S_{yy} \end{bmatrix} \equiv \begin{bmatrix} \dfrac{\partial u_x}{\partial x} & \dfrac{1}{2}\left[\dfrac{\partial u_x}{\partial y}+\dfrac{\partial u_y}{\partial x}\right] \\ \dfrac{1}{2}\left[\dfrac{\partial u_x}{\partial y}+\dfrac{\partial u_y}{\partial x}\right] & \dfrac{\partial u_y}{\partial y} \end{bmatrix}$$
$$= \begin{bmatrix} \phi_{xy} & \tfrac{1}{2}(\phi_{yy}-\phi_{xx}) \\ \tfrac{1}{2}(\phi_{yy}-\phi_{xx}) & -\phi_{xy} \end{bmatrix}. \tag{2.5}$$

The *principal strain rate* is
$$S(\boldsymbol{R}) \equiv \sqrt{(-\det S_{ij})} = \tfrac{1}{2}(C_1-C_2). \tag{2.6}$$

The *persistent strain rate*, defined by Frank & Mackley (1976) as the strain rate of a non-rotating fluid line at $\boldsymbol{R}$, is
$$\sigma(\boldsymbol{R}) = \sqrt{(S^2(\boldsymbol{R})-\omega^2(\boldsymbol{R}))} = \sqrt{(-C_1C_2)}. \tag{2.7}$$

Obviously σ is real only where the Gaussian curvature of ϕ is negative.

The *lines of curvature* of ϕ form an orthogonal net of fluid lines that are momentarily not altering in length. They are rotating, however, with angular velocities
$$\omega_1 = -C_1, \quad \omega_2 = -C_2, \tag{2.8}$$

where the subscripts on ω refer to the fluid lines along which the surface has the corresponding principal curvatures, and where a positive ω has angular velocity vector along $\hat{\boldsymbol{z}}$. The net of lines of curvature divides the region near any point $\boldsymbol{R}$ into two pairs of opposite quadrants. Fluid lines issuing from $\boldsymbol{R}$ into one pair of quadrants are momentarily extending, while those issuing into the other pair are contracting. If the Gaussian curvature of ϕ is negative, ω_1 and ω_2 have opposite sign and fluid lines along both directions of curvature are rotating into the extending quadrants, which contain the non-rotating lines whose strain rate is σ. The *strain rate trajectories*, defined by the directions of the principal axes of S_{ij}, also form an orthogonal net oriented at 45° to the net of lines of curvature. Figure 1 shows the two nets and the streamlines near a hyperbolic critical point; fluid lines along the outgoing streamlines remain in the extending quadrants for arbitrarily long times and hence 'persistently extend' with strain rate σ.

The singular flow which is the principal object of study in this paper belongs to a class of flows where $2n$ alternately outgoing and ingoing streamlines issue symmetrically from a degenerate critical point at $R = 0$. The flow function is
$$\phi(\boldsymbol{R}) = (\gamma/n)\,\mathrm{Re}\,(x+\mathrm{i}y)^n = (\gamma R^n/n)\cos n\theta, \tag{2.9}$$

where (R, θ) are the polar coordinates of $\boldsymbol{R}$ and γ is a constant. This flow is irrotational. When $n = 2$ the critical point is in fact not degenerate but hyperbolic, and the flow closely approximates that in a four roll mill (Crowley *et al.* 1976). For general n the flow is expected to approximate that in a '$2n$ roll mill' whose rollers are alternately counter rotating about parallel axes

PHILOSOPHICAL TRANSACTIONS OF THE ROYAL SOCIETY A MATHEMATICAL, PHYSICAL & ENGINEERING SCIENCES

forming a prism whose normal cross-section is a regular $2n$ sided polygon. The general case will not be studied here, because the form of the perturbation of $\phi(\boldsymbol{R})$ that would 'unfold' the singularity at $\boldsymbol{R} = 0$ in all possible topologically distinct ways is not known. When $n = 3$, however, the universal unfolding is known and attention will henceforth be restricted to this case.

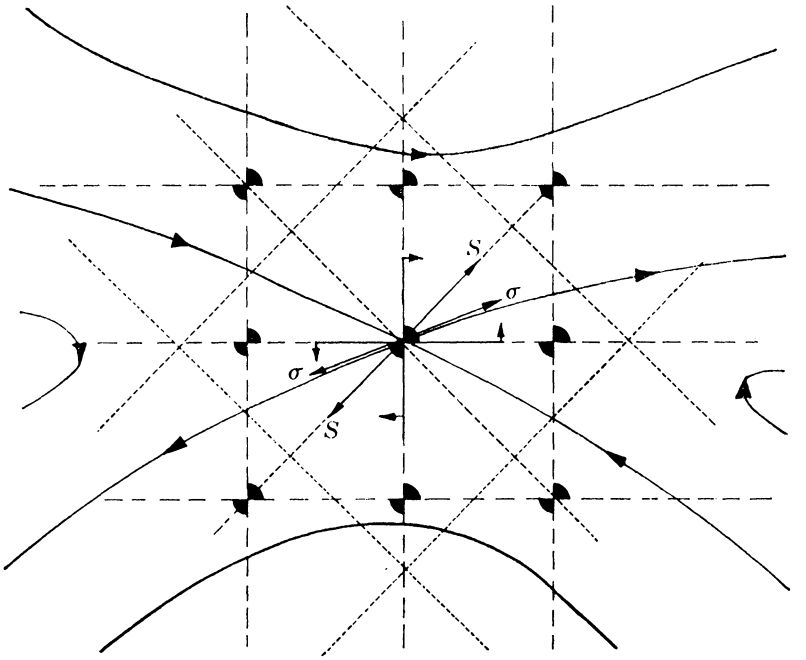

FIGURE 1. Streamlines (—▶—), lines of curvature (— — —) and strain rate trajectories (– – – –) near a hyperbolic critical point. Extending quadrants are shaded (◔) and the directions of extension and rotation of fluid lines are marked with light arrows. S is the principal strain rate and σ the persistent strain rate.

The flow given by equation (2.9) when $n = 3$ contains only cubic terms in its stream function ϕ. This suggests that the universal unfolding contains the 'missing' linear and quadratic terms in x and y, and it is plausible on physical grounds that these terms correspond to the addition to the singular flow of a uniform translational flow with velocity $\boldsymbol{V} = (V_x, V_y, 0)$ and a uniform vorticity $\omega\hat{\boldsymbol{z}}$. The stream function now becomes

$$\phi(\boldsymbol{R}) = \gamma(\tfrac{1}{3}x^3 - xy^2) - \tfrac{1}{2}\omega(x^2+y^2) - V_y x + V_x y. \tag{2.10}$$

It was proved by Arnol'd (1973) that this is in fact the universal unfolding of the singular flow: any further perturbation may deform the streamlines but cannot change the topology of the critical-point structure of the totality of flows obtained from equation (2.10) by varying ω, V_x and V_y. Precisely the stream function (2.10) appears as the 'elliptic umbilic catastrophe' in the classification of Thom (1972). In the language of catastrophe theory, x and y are 'state variables', ω/γ, V_x/γ and V_y/γ are 'control parameters' and $\frac{1}{3}x^3 - xy^2$ is the 'germ' of the catastrophe. These aspects of the flow will be further discussed in § 3.

For large R the flow (2.10) has outgoing streamlines in directions $\theta = 90°$, $210°$ and $-30°$, and incoming streamlines in directions $\theta = 30°$, $150°$ and $270°$. This suggests that the flow will be closely approximated in the central region of a six roll mill with rollers arranged as on figure 2. The rollers, which have radius a and separation d–a, rotate in the senses shown, and the rotation rates Ω_1 to Ω_6 are positive quantities by definition.

The control parameters ω/γ and V/γ in the stream function ϕ of equation (2.10) depend on the roller rates Ω_1 to Ω_6 in a manner that can be determined by a matching procedure on the assumption that ϕ gives a good approximation to the flow up to the inner surfaces of the rollers as well as for small R. Consider first the case $V = 0$. This can be realized by making the three anticlockwise roller speeds Ω_1, Ω_3 and Ω_5 the same (Ω_A, say), and the three clockwise roller rates Ω_2, Ω_4 and Ω_6 the same (Ω_B, say). By matching the speeds $a\Omega_A$ and $a\Omega_B$ of the rollers' peripheries (c.f. figure 2) to the flow velocities $\boldsymbol{u}$ generated by (2.1) and (2.10) at their inner surfaces $R = d, \theta = 0, \pi/3 \ldots 5\pi/3$, it is not hard to obtain the following expressions for γ and ω:

$$\gamma = (a/2d^2)\,(\Omega_A+\Omega_B), \quad \omega = (a/2d)\,(\Omega_B-\Omega_A). \tag{2.11}$$

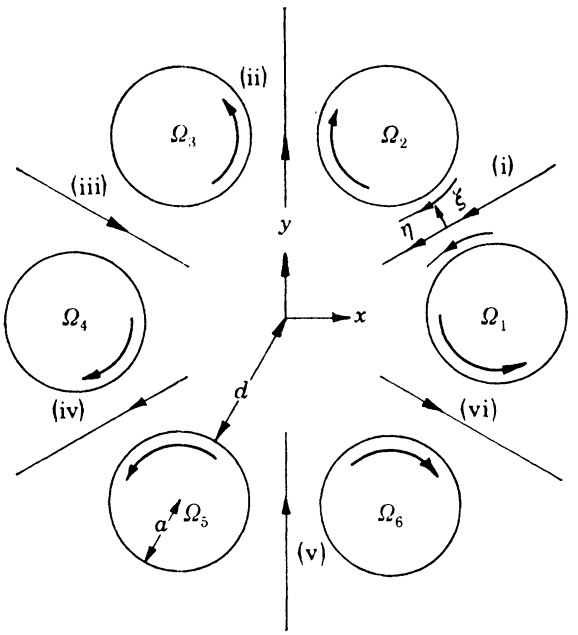

FIGURE 2. Six roll mill geometry. Rollers are labelled 1 to 6 and streams between rollers are labelled (i) to (vi). ξ and η are coordinates describing the approximately two roll mill flow in stream (i).

In the general case this method fails, but the expressions just found suggest that γ and ω are respectively proportional to the mean roller rate $\bar{\Omega}$ and the difference $\Delta\Omega$ of the mean rates of the clockwise and anticlockwise rollers, that is

$$\gamma = a\bar{\Omega}/d^2, \quad \omega = a\Delta\Omega/2d, \tag{2.12}$$

where

$$\left.\begin{aligned} \bar{\Omega} &\equiv \tfrac{1}{6}(\Omega_1+\Omega_2+\Omega_3+\Omega_4+\Omega_5+\Omega_6), \\ \Delta\Omega &\equiv \tfrac{1}{3}(\Omega_2+\Omega_4+\Omega_6-\Omega_1-\Omega_3-\Omega_5). \end{aligned}\right\} \tag{2.13}$$

The velocity parameters V_x and V_y can be estimated by representing the flow near $\boldsymbol{R} = 0$ as the superposition of six two roll mill flows corresponding to the streams (i) to (vi). Employing the coordinates (ξ, η) shown on figure 2 to describe the flow between rollers 1 and 2, the stream function may be taken to be

$$\phi(\xi,\eta) = \frac{-\int_0^{\xi} u_{(1)}(\xi')\,\mathrm{d}\xi'}{1+(\eta^2/a(d-a))}, \qquad \left.\begin{aligned} u_{(1)}(d-a)/2 &= a\Omega_2, \\ u_{(1)}(a-d)/2 &= a\Omega_1. \end{aligned}\right\} \tag{2.14}$$

This has the following properties: (*a*) $u_{(i)}(\xi)$ is the velocity profile across the 'throat', $\eta = 0$, of stream (i), matched to the roller speeds at $(\xi) = (d-a)/2$. (*b*) The straight line $\xi = 0$ is a streamline. (*c*) When $\Omega_1 = \Omega_2$ and $u_{(i)}(\xi)$ is a constant the streamlines form a family of parabolae whose curvature at $(\xi) = (d-a)/2$ matches that of the rollers.

At the centre of the six roll mill the stream (i) contributes a velocity

$$\boldsymbol{u}_{(i)}(\boldsymbol{R} = 0) = \frac{u_{(i)}(\xi = 0)}{1 + \dfrac{3(d+a)^2}{4a(d-a)}}\,\hat{\boldsymbol{\eta}}, \tag{2.15}$$

where $\hat{\boldsymbol{\eta}}$ is the unit vector in the η direction. It is reasonable to assume that $u_{(i)}(\xi = 0)$ will be proportional to the mean of the peripheral roller speeds $a\Omega_1$ and $a\Omega_2$. The constant of proportionality will be taken as α_+ for the inflowing streams (i), (iii) and (v) and α_- for the outflowing streams (ii), (iv) and (vi). As will be further discussed in §6, the difference between α_+ and α_- is of crucial importance in understanding the streamline patterns of flowing polymer solution. The control parameters V_x and V_y of the flow (2.10) are just the components of the velocity $\boldsymbol{u}(\boldsymbol{R} = 0)$, and summing the six stream contributions of the type (2.15) gives

$$\left.\begin{aligned} V_x &= \frac{\sqrt{3}a}{4\left[1 + \dfrac{3(d+a)^2}{4a(d-a)}\right]}\,[\alpha_+(\Omega_3+\Omega_4-\Omega_1-\Omega_2) - \alpha_-(\Omega_4+\Omega_5-\Omega_1-\Omega_6)], \\ V_y &= \frac{a}{4\left[1 + \dfrac{3(d+a)^2}{4a(d-a)}\right]}\,[\alpha_+(2\Omega_5+2\Omega_6-\Omega_1-\Omega_2-\Omega_3-\Omega_4) \\ &\qquad + \alpha_-(2\Omega_2+2\Omega_3-\Omega_1-\Omega_4-\Omega_5-\Omega_6)]. \end{aligned}\right\} \tag{2.16}$$

3. Elliptic umbilic catastrophe

As the roller speeds are varied, the parameters γ, ω, $\boldsymbol{V}$ of the stream function $\phi(\boldsymbol{R})$ of equation (2.10) change according to equations (2.12) and (2.16), and the different flows of the family can be explored. Of particular interest are the singular flows, whose critical points are degenerate, that is $S = \omega$ where $\boldsymbol{u} = 0$. Equations (2.5) and (2.6) give the principal strain rate of ϕ as

$$S = 2\gamma R. \tag{3.1}$$

The vorticity is uniform for the flows under consideration, and this means that the degenerate critical points must lie on the circle $R = \omega/2\gamma$. Since the critical points for any γ, ω, $\boldsymbol{V}$ are completely determined by the vanishing of $\nabla\phi$, the existence of a singular flow implies a relation between the control parameters. In fact singular flows lie on a 'catastrophe surface' Σ in the 'control space' whose coordinates are ω/γ, V_x/γ and V_y/γ. The equation of Σ, parameterized by a variable θ, is

$$V_x/\gamma = (\omega/\gamma)^2 \sin\theta\,\tfrac{1}{2}(1+\cos\theta), \quad V_y/\gamma = (\omega/\gamma)^2\,\tfrac{1}{2}(\cos^2\theta - \cos\theta - \tfrac{1}{2}). \tag{3.2}$$

The surface Σ is illustrated on figure 3; its sections for constant ω are deltoid curves with linear dimensions proportional to ω^2. To each point P in the control space there corresponds a flow with a pattern of streamlines in the $\boldsymbol{R}$ plane. If P lies outside Σ the flow has two non-degenerate critical points, both hyperbolic. If P lies within Σ the flow has four non-degenerate critical points, three hyperbolic and one elliptic. Therefore as P crosses Σ from the inside a hyperbolic and an elliptic critical point must annihilate. These are the 'catastrophes'.

There are three sorts of catastrophe in the flow family under consideration. The simplest is the 'fold', where P pierces the smooth surface of Σ, as in the sequence of positions labelled

5, 4, 3 on figure 3; the annihilation of critical points takes place as shown on figure 4*a*. The next simplest is the 'cusp', where P pierces a cusp edge of Σ, as in the sequence 7, 8, 9 on figure 3; the annihilation now involves an extra hyperbolic critical point as shown on figure 4*b*. The third sort of catastrophe is the elliptic umbilic itself, where P passes through the singular point $\omega = 0$, $V = 0$ of Σ, as in the sequence 2, 1, 10 on figure 3; the annihilation involves two extra hyperbolic points and will be studied later (see figure 7, plates 2 and 3).

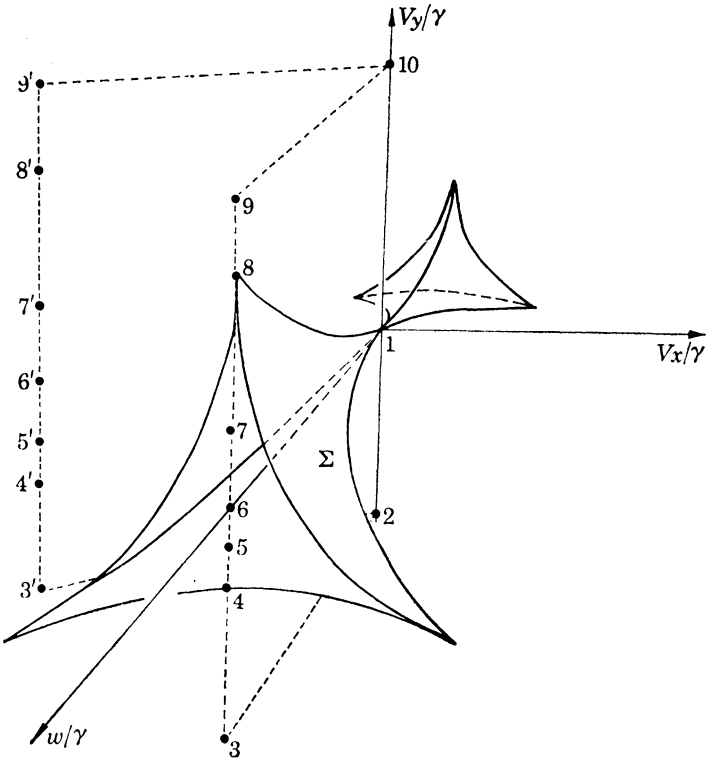

FIGURE 3. Elliptic umbilic catastrophe surface Σ in control space.
The numbers correspond to flows on figures 7 and 8.

The nature of the persistent extension of fluid lines is different for different sorts of critical point. It is conveniently described by the *extension index* ν defined as follows: let r measure distance from the critical point along an outgoing streamline issuing from it. Then for small r the fluid speed is

$$u(r) = kr^{\nu}, \tag{3.3}$$

where k is constant. Alternatively stated, an infinitesimal fluid line of length l_0 at r_0, on and parallel to the streamline, extends to length l at r, and

$$l/l_0 = (r/r_0)^{\nu}. \tag{3.4}$$

Employing the standard forms of catastrophe stream function ϕ as given by Thom (1972), it is possible to calculate ν for the types of critical point considered in this paper, with the following results

$$\nu = \left\{ \begin{array}{l} 1 \text{ (hyperbolic critical point)}, \\ \frac{3}{2} \text{ (fold catastrophe critical point as in figure 4}a\text{)}, \\ 2 \text{ (cusp catastrophe critical point as in figure 4}b\text{)}, \\ 2 \text{ (elliptic umbilic critical point as in figure 7, plates 2 and 3)}. \end{array} \right\} \tag{3.5}$$

Near a critical point the persistent strain rate σ varies as $r^{\nu-1}$. At a degenerate critical point σ vanishes, and from (2.7) the Gaussian curvature of ϕ vanishes too. Therefore one or both principal curvatures must vanish. At fold and cusp critical points just one curvature vanishes, and the streamlines through these points touch the corresponding line of curvature (along which the fluid line does not rotate, as equation 2.8 shows). At the elliptic umbilic critical point of the flow (2.10) ($\omega = 0$, $\boldsymbol{V} = 0$ in control space and $\boldsymbol{R} = 0$ in state space) both curvatures vanish,

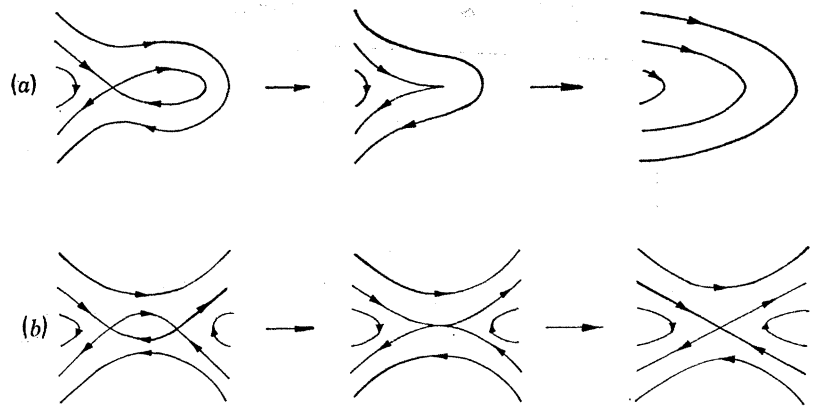

FIGURE 4. Sequence of flow patterns in unfolding of (*a*) fold catastrophe (corresponding to the sequence 543 on figure 3), (*b*) cusp catastrophe (corresponding to the sequence 789 on figure 3).

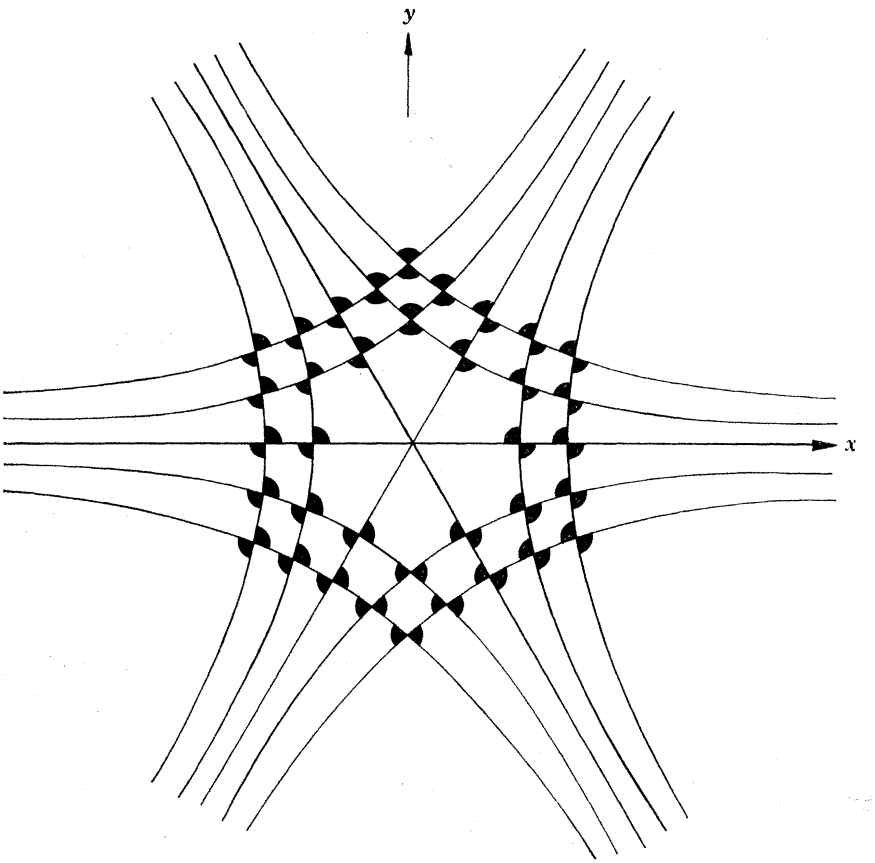

FIGURE 5. Net of lines of curvature for elliptic umbilic flow field. Extending quadrants are shaded ( ).

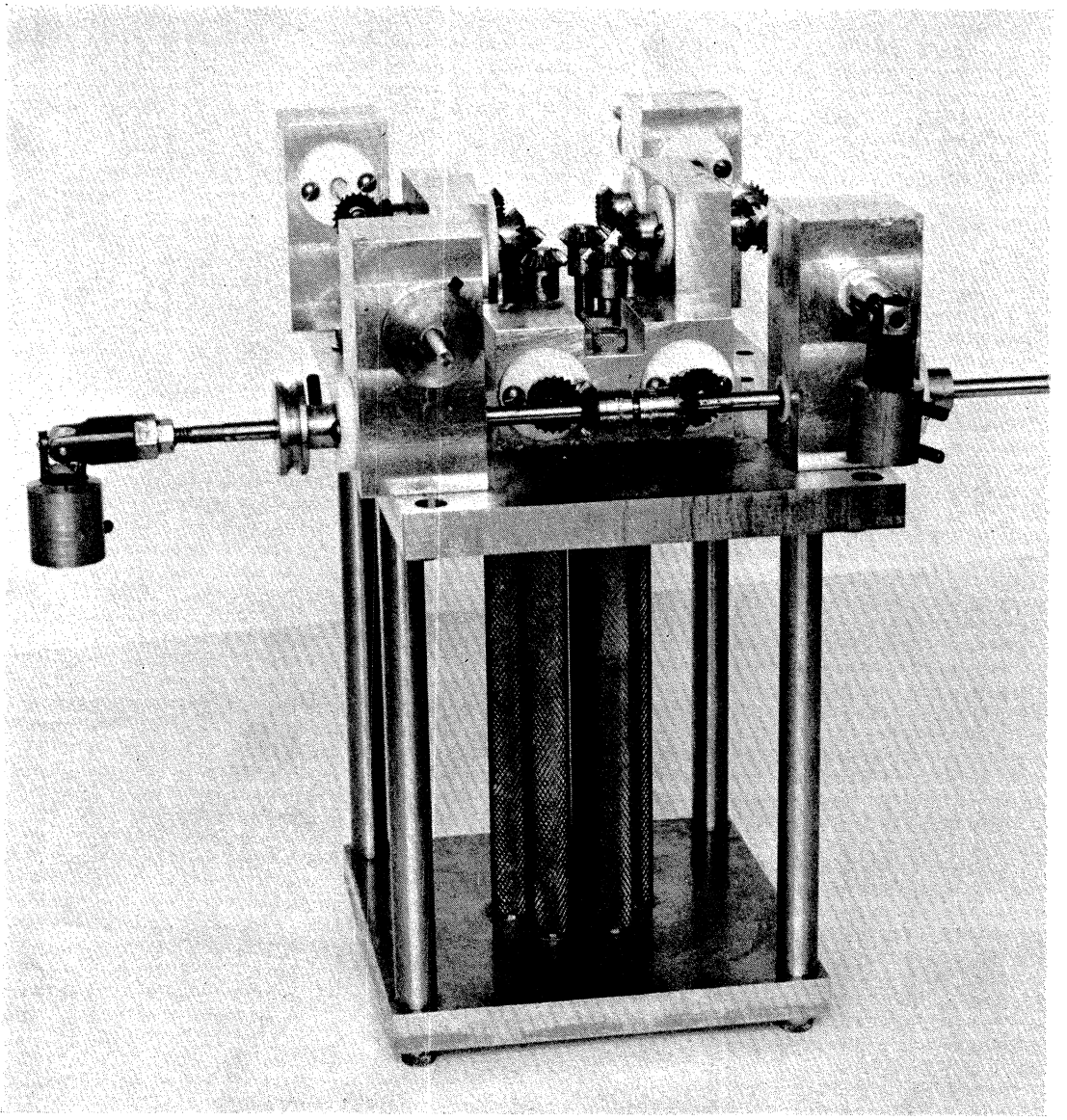

FIGURE 6. Photograph of six roll mill.

(*Facing p.* 8)

PHILOSOPHICAL TRANSACTIONS OF THE ROYAL SOCIETY A MATHEMATICAL, PHYSICAL & ENGINEERING SCIENCES

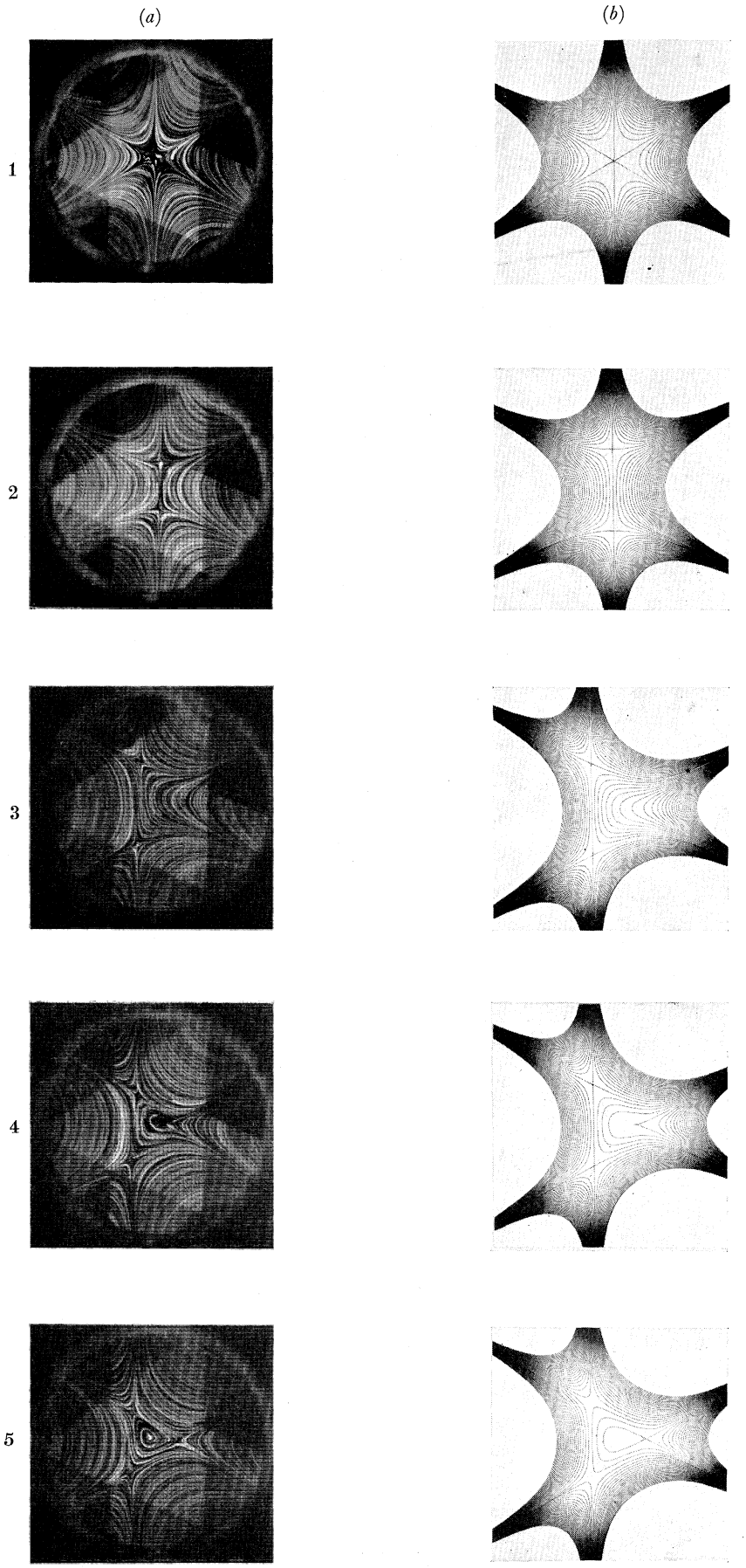

FIGURE 7. For description see opposite.

PHILOSOPHICAL TRANSACTIONS OF THE ROYAL SOCIETY A MATHEMATICAL, PHYSICAL & ENGINEERING SCIENCES

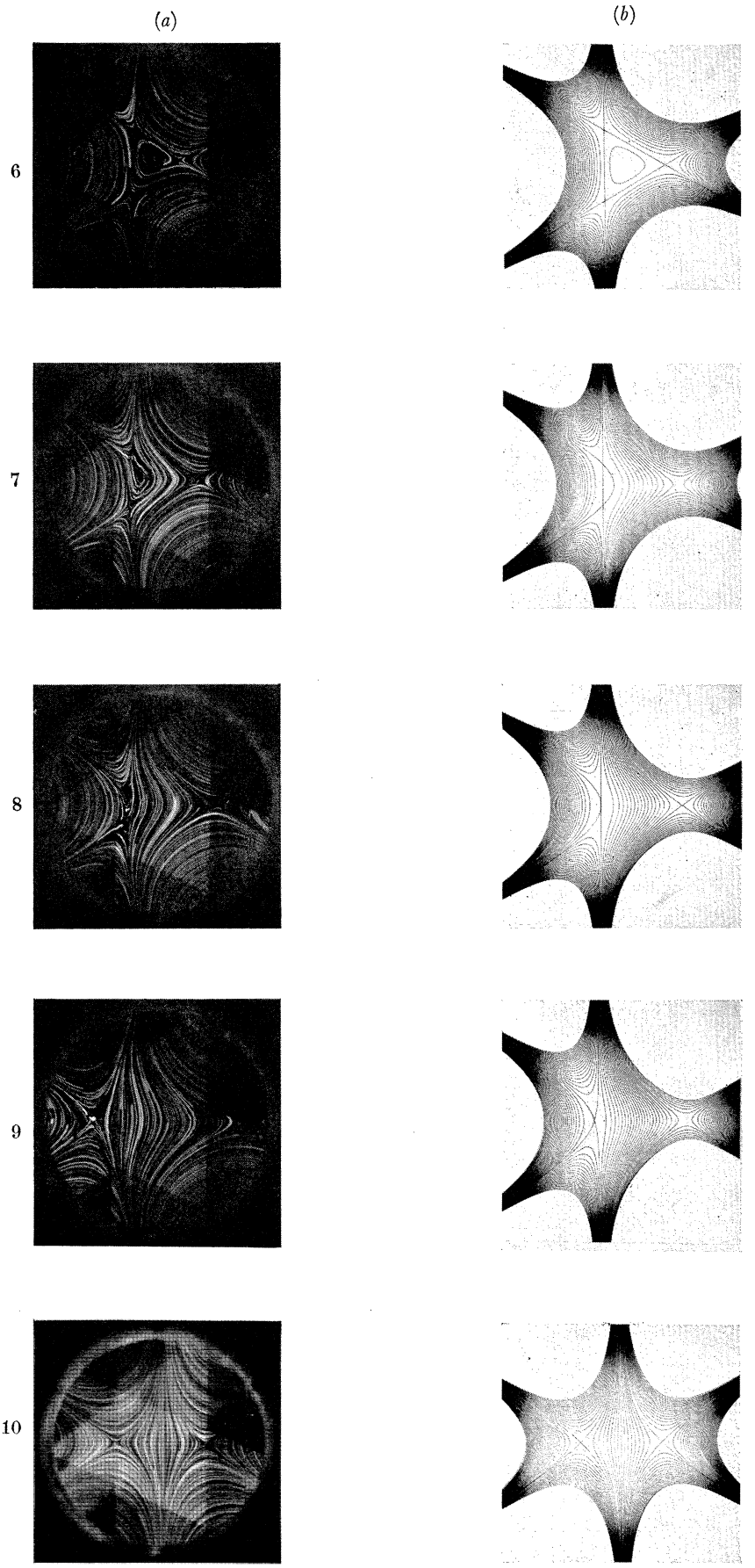

FIGURE 7. (*a*) Flows 1 to 10 of glycerol in the six roll mill, corresponding to roller speeds Ω_{I}, Ω_{II} and Ω_{III} of table 1. (*b*) Computer simulations of flows 1 to 10 with control parameters ω/γ and V_y/γ of table 1.

PHILOSOPHICAL TRANSACTIONS OF THE ROYAL SOCIETY A MATHEMATICAL, PHYSICAL & ENGINEERING SCIENCES

FIGURE 8. For description see opposite.

PHILOSOPHICAL TRANSACTIONS OF THE ROYAL SOCIETY A MATHEMATICAL, PHYSICAL & ENGINEERING SCIENCES

FIGURE 8. Streamline patterns of (*a*) glycerol and (*b*) 2% polyethylene oxide solution in the six roll mill corresponding to roller speeds Ω_{I}, Ω_{II} and Ω_{III} of table 2. (*c*) Corresponding flow birefringence observations of the polyethylene oxide solution.

PHILOSOPHICAL TRANSACTIONS OF THE ROYAL SOCIETY A MATHEMATICAL, PHYSICAL & ENGINEERING SCIENCES

since when $\omega = 0$ the vanishing of σ implies the vanishing of S (equation 2.7) and this in turn implies $C_1 = C_2 = 0$ (equation 2.6). A point on a surface where both curvatures are equal (so that $S = 0$) is called an 'umbilic point'; the directions of principal curvature are not defined there, and the net of lines of curvature is singular. Figure 5 shows this net for the stream function (2.10); the lines are independent of the control parameters, and are determined by the equations

$$\tan 2\phi = -\tan\theta, \tag{3.6}$$

where ϕ is the direction of the lines at points $\boldsymbol{R}$ with polar angle θ. The singularity at the umbilic point at the origin is evident.

4. Streamline patterns for Newtonian fluid

A six roll mill was constructed. The rollers were 120 mm in length. In the experiments to be described two sets of rollers were used. Referring to figure 2, their respective dimensions were $a_1 = 3$ mm, $d_1 = 12$ mm, and $a_2 = 4.5$ mm, $d_2 = 10.5$ mm; the latter set of rollers were given a cross knurled finish. Three independent electric motors were connected with gears to three pairs of rollers with speeds Ω_{I}, Ω_{II}, Ω_{III} arranged as follows

$$\left.\begin{aligned} \Omega_{\mathrm{I}} &= \Omega_3 = \Omega_5, \\ \Omega_{\mathrm{II}} &= \Omega_1 = \Omega_4, \\ \Omega_{\mathrm{III}} &= \Omega_2 = \Omega_6. \end{aligned}\right\} \tag{4.1}$$

The speed of each set of rollers could be independently varied and the rotation rate of each monitored. Figure 6, plate 1 is a photograph of the mill showing the essential features of the mechanism.

In the first series of experiments the rollers of the mill were immersed in glycerol which was contained in a cylindrical tank (diameter = 150 mm) with an optical flat bottom surface. Streamline patterns were made visible by illuminating the regions between the rollers with a horizontal plane beam of light and including a small quantity of polyethylene powder into the glycerol to act as scattering centres. Photographs of the streamlines produced by the scattering particles were taken from below; typical exposure times were of the order one second.

In this series of experiments the smaller diameter rollers were chosen $a_1 = 3$ mm, $d_1 = 12$ mm, in order that the gap between the rollers was sufficiently large to be able to illuminate a significant proportion of the region within the mill. Illumination was provided by a mercury lamp. The plane beam was split by a system of mirrors into three components and directed into the mill through streams (iv), (v) and (vi) indicated in figure 2. The gap width of the rollers can be identified on the streamline photographs by the clearly defined width of the illuminated regions. The diameter of the observed field of view in all the streamline photographs was 18 mm, a limit set by the size of the central hole in the bottom plate of the mill. Ten flows were studied corresponding to the roller speeds shown in table 1. Figure 7(1*a*–10*a*), plates 2 and 3, shows photographs of the streamline patterns in these flows. Degenerate critical points can be seen on flows 1 (elliptic umbilic), 4 (fold, c.f. figure 4*a*) and 8 (cusp, c.f. figure 4*b*).

Figure 7*a* suggests that the flows 1 to 10 correspond to a sequence of points in control space that are situated relative to the catastrophe surface Σ as indicated by the numbers on figure 3. This hypothesis can be tested by computer simulation of the stream lines as contours of the

PHILOSOPHICAL TRANSACTIONS OF THE ROYAL SOCIETY A MATHEMATICAL, PHYSICAL & ENGINEERING SCIENCES

model stream function (2.10). The control variables can be calculated from equations (4.1) (2.12) and (2.16), which give

$$\left.\begin{aligned} \omega/\gamma &= \frac{d(\Omega_{\mathrm{III}}-\Omega_{\mathrm{I}})}{\Omega_{\mathrm{I}}+\Omega_{\mathrm{II}}+\Omega_{\mathrm{III}}}, & (a)\\ V_x/\gamma &= \frac{3\sqrt{3}\,d^2(\alpha_+-\alpha_-)\,(\Omega_{\mathrm{I}}-\Omega_{\mathrm{III}})}{4[1+3(d+a)^2/4a(d-a)]\,(\Omega_{\mathrm{I}}+\Omega_{\mathrm{II}}+\Omega_{\mathrm{III}})}, & (b)\\ V_y/\gamma &= \frac{3d^2(\alpha_++\alpha_-)\,(\Omega_{\mathrm{I}}+\Omega_{\mathrm{III}}-2\Omega_{\mathrm{II}})}{4[1+3(d+a)^2/4a(d-a)]\,(\Omega_{\mathrm{I}}+\Omega_{\mathrm{II}}+\Omega_{\mathrm{III}})}. & (c) \end{aligned}\right\} \tag{4.2}$$

TABLE 1. DATA FOR FLOWS NUMBERED 1 TO 10 ON FIGURE 3 AND FIGURE 7

Ω_{I}, Ω_{II} and Ω_{III} are the experimental roller speeds in radians per second (each value of Ω has an estimated error of $\pm 6\,\%$). ω/γ and V_y/γ (with $V_x = 0$) are the control parameters employed in the computer simulation of the flows.

flow no.	1	2	3	4	5	6	7	8	9	10
Ω_{I}	2.5	2.5	1.0	1.0	1.0	1.0	1.0	1.0	1.0	2.5
Ω_{II}	2.5	4.0	4.0	3.0	2.5	2.25	1.25	0.5	0	0.5
Ω_{III}	2.5	2.5	4.0	4.0	4.0	4.0	4.0	4.0	4.0	2.5
ω/γ	0	0	1	1	1	1	1	1	1	0
V_y/γ	0	-1	$-\frac{1}{2}$	$-\frac{1}{4}$	$-\frac{1}{8}$	0	$\frac{1}{2}$	$\frac{3}{4}$	1	1

Glycerol is, to a good approximation, a Newtonian fluid, and there is no reason why flows in the incoming and outgoing streams should have different velocity fields. Therefore the multipliers α_+ and α_- introduced after equation (2.15) may be set equal (to α, say). According to equation (4.2b) this implies that $V_x = 0$, so that all flows should lie in the (ω, V_y) plane in control space. This suggests a quantitative test of the model stream function that is independent of the mill dimensions and the value of the multiplier α. It follows from equations (3.2) that the ratio of the quantities

$$q \equiv \frac{(V_y/\gamma)}{(\omega/\gamma)^2} \tag{4.3}$$

for the cusp and fold points (8 and 4 on figure 3) should be -3. The experimental value of this ratio, calculated from equations (4.2a, c) and the roller speeds of table 1 is -2.75, in fair agreement with the theoretical value. For α this method gives $\alpha = 1.42 \pm 0.06$ (With the larger rollers the ratio of quantities q comes out as -3.4, and $\alpha = 0.48 \pm 0.03$.)

For a visual comparison of actual and model flows the control parameters ω/γ, V_y/γ of table 1 were employed, and contours of the stream function (2.10) computed for flows 1 to 10. These are shown on figure 7 (1b–10b), plates 2 and 3. The agreement is remarkably good, even out towards the rollers whose inner surfaces lie outside the periphery of figure 7a, plates 2 and 3.

An interesting feature was observed that reflects the nature of the elliptic umbilic catastrophe surface near the origin of control space. It was observed experimentally that flows near the origin of control space were very much more sensitive to changes in V_y/γ (equation 4.2c) than to comparable changes in ω/γ (equation 4.2a); this is fully consistent with the manner in which the cross section of Σ (figure 3) shrinks to a point as ω vanishes.

5. Streamline patterns for polymer solution

In the second series of experiments streamline patterns were studied with glycerol (for comparison) and a 2 % solution of polyethylene oxide (WSR 301) in water, to discover how the flows are affected by extending polymer chains in the outgoing streams.

For these experiments the larger roller diameter was chosen, $a_2 = 4.5$ mm, $d_2 = 10.5$ mm. This was done in order to obtain increased magnitudes for the persistent strain rate for any given rotation rate of the rollers. This enabled flow birefringence observations to be made. In addition, it was also found necessary to knurl the rollers to prevent suspected 'slipping' at the rollers when polymer solutions were used.

Figure 8(1*a*–10*a*), plates 4 and 5, show the behaviour of glycerol for the ten flows studied with roller speeds shown in table 2. As expected the topology of the flows follows that of the previous figure 7(1*a*–10*a*), plates 2 and 3, where smaller diameter rollers were used. Figure 8(1*b*–10*b*), plates 4 and 5, are photographs of the streamline patterns for a 2 % solution of polyethylene oxide in water, the corresponding roller speeds are again given in table 2. This sequence of flows is strikingly different from that obtained with glycerol. All flows except the symmetrical flow 1 possess two hyperbolic critical points; there are no elliptic critical points as with flows 5, 6 and 7 on figure 7, plates 2 and 3 and no degenerate fold and cusp critical points as with flows 4 and 8 on figure 7, plates 2, and 3. It appears, however, that the flows 1, 2 and 10 are substantially the same with polymer solution and glycerol.

Table 2. Data for flows numbered 1 to 10 on figure 8

Ω_{I}, Ω_{II}, Ω_{III} are the experimental roller speeds for each series (8*a*, 8*b* and 8*c*) corresponding to each flow number (each value of Ω has an estimated error of $\pm 6\,\%$).

flow no.	1	2	3	4	5	6	7	8	9	10
Ω_{I}	2.5	2.5	2.0	2.0	2.0	2.0	2.0	2.0	2.0	2.5
Ω_{II}	2.5	4.0	4.0	3.5	2.75	2.0	1.0	0.5	0	0.5
Ω_{III}	2.5	2.5	4.0	4.0	4.0	4.0	4.0	4.0	4.0	2.5

The first step towards understanding this behaviour is the observation that the flows 3, 4 ... 9 where polymer solution differs from glycerol are those for which the vorticity ω is non-zero (cf. figure 3). The second step is the observation that the change in the polymer streamlines from flow 2 to flow 10 consists of a smooth counterclockwise rotation of the line joining the two hyperbolic critical points from the y axis to the x axis. This strongly suggests that with polymer the sequence of flows explored is not 1 2 3 4 5 6 7 8 9 10 but a different sequence, such as that shown as 1 2 3′ 4′ 5′ 6′ 7′ 8′ 9′ 10 on figure 3, in which the arc 3 ... 9 has swung out of the (V_y, ω) plane to avoid intersecting Σ. It is simple to confirm that a swing towards negative V_x is required for the line joining the two hyperbolic points to rotate in the sense observed.

It seems that the same roller speeds which produce no velocity component V_x with glycerol produce a negative V_x with polymer. This can be explained by equation (4.2) on the assumption that $\alpha_+ > \alpha_-$ for polymer solution, because then V_x is proportional to $-\omega$, corresponding to points on the dotted path in figure 3 that does not intersect Σ. Recalling the definition of α_+ and α_- following equation (2.15), this implies that fluid in the central streamlines between pairs of rollers moves faster in the inflowing streams than in the outflowing streams.

This is reasonable. The central streamlines presumably lie close to the asymptotic streamlines issuing from critical points of the flow field. On outgoing asymptotic streamlines the flow is

persistently extensional and stretches polymer chains dissolved in the flow as shown by birefringence observations reported in §6. The sheet of highly extended chains inhibits the development of high strain rates, as suggested by an experiment of Frank & Mackley (1976). This in turn reduces the flow velocity on the outgoing asymptotic streamlines far from the critical point. No such effect is expected for the inflowing streams so that α_+ should exceed α_- as the flow patterns suggest.

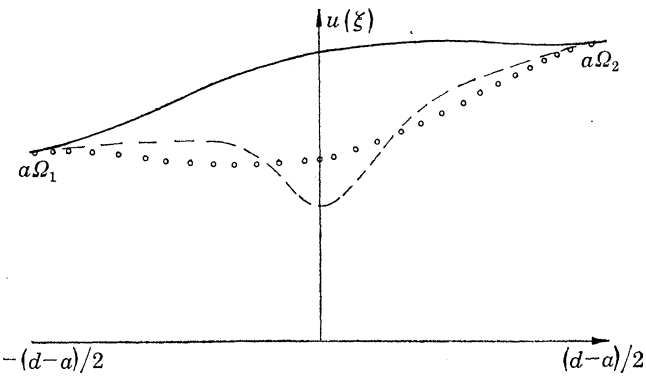

FIGURE 9. Conjectured velocity profiles $u(\xi)$ between adjacent rollers with rotation rates Ω_1 and Ω_2. The full line is for a Newtonian fluid, the dashed line is for outflowing polymer solution and the dotted line is for inflowing polymer solution.

The elliptic umbilic family of flows is a very sensitive indicator of polymer-induced modification of the velocity field, because Σ shrinks to zero thickness as the vorticity vanishes, and the slightest asymmetry $\alpha_+ - \alpha_-$ between inflows and outflows will swing the sequence of control points away from Σ. Professor T. Poston has pointed out to us that this reflects the fact that Ω_{I}, Ω_{II} and Ω_{III} correspond to two and not three elliptic umbilic control variables, since multiplying all roller speeds by the same factor merely intensifies the flow without changing the streamlines. The third essential control variable is $\alpha_+ - \alpha_-$ which corresponds to adding polymer. Furthermore, some of the flow patterns without polymer (figures 7 and 8*a*), plates 2, 3, 4 and 5), which all have $V_x = 0$, possess the non-generic property of *saddle connections*, that is streamlines joining two saddles; when polymer is added to flows with vorticity, making $\alpha_+ \neq \alpha_-$ and $V_x \neq 0$, the saddle connections are destroyed as figure 8*b*, plates 4 and 5 shows.

It is of course necessary that the total outgoing flux in all six streams always vanishes. When considered together with the asymmetry under discussion this has implications for the velocity profiles $u(\xi)$ between pairs of rollers (cf. equation 2.14). Between rollers with rotation rates Ω_1 and Ω_2 (e.g. stream (i) on figure 2) $u(\xi)$ must change smoothly from $a\Omega_1$ when $\xi = -\frac{1}{2}(d-a)$ to $a\Omega_2$ when $\xi = \frac{1}{2}(d-a)$, whatever fluid is in the mill and whether the stream flows out or in. With polymer, however, the sheets of extended chains in the outflows will act as a barrier, considerably reducing $u(\xi)$ near $\xi = 0$ in comparison with speeds in the flow with Newtonian fluid (figure 9). Therefore the flux in an outgoing polymer stream will be less than that in a corresponding Newtonian flow. The barrier in the outflow will cause the pressure in the central region of the mill to rise and in turn reduce the fluxes in the incoming polymer stream to balance those in the outgoing streams. In the inflows, however, there need be no sharp diminution in speed near $\xi = 0$ and it is probable that the reduction in $u(\xi)$ is more smoothly distributed over the cross section of the streams, as indicated in figure 9.

6. Flow birefringence

It is now established (Mackley & Keller 1975; Crowley *et al.* 1976; Frank & Mackley 1976) that localized extension of polymer chains in persistently extensional flows can be detected by the birefringence it produces in the fluid, on observing the illuminated flow through crossed polarizer and analyser. For the flows of figure 8(1*b*–10*b*), plates 4 and 5, the flow birefringence was photographed while continuously rotating the polarizer and analyser so as to ensure recording the intensity of the birefringence irrespective of its orientation. Photographic exposure times were of the order 3 seconds; other aspects of the experimental technique were essentially as described in Crowley *et al.* (1976). The result was the series of pictures shown on figure 8(1*c*–10*c*), plates 4 and 5.

The observed flow birefringence is sharply localized near the outgoing streamlines issuing from critical points. As explained by Crowley *et al* (1976), the reason for this is that only near these streamlines do polymer chains reside in the flow for long enough to get fully extended. For each given position in control space comparison of the position of the localized birefringence with each associated flow pattern, figure 8(1*b*–10*b*), plates 4 and 5 shows that the birefringence occurs consistently as 'birefringent sheets of oriented molecules' along streamlines issuing from critical points. The 'width' of the birefringent sheet is also consistent with that previously observed for a single hyperbolic critical point (Crowley *et al.* 1976). However, in contrast to flow configurations studied previously, the intensity of birefringence along the asymptotic streamlines is clearly far from uniform: there is a sharp diminution of intensity towards the centre of the flow field. This effect is most marked on figure 8(1*c*), plate 4.

It was also noted that the birefringence intensity was somewhat time dependent. When flows were changed from one setting in control space to another it was observed that the intensity of the localized birefringence would decay from an initial essentially uniform distribution along the asymptotic streamline to the 'equilibrium' distribution which is weak near $\boldsymbol{R} = 0$.

To understand the weak birefringence near $\boldsymbol{R} = 0$, observe that no hyperbolic critical points can exist within the circle $R = \omega/2\gamma$ where the flow is vorticity dominated (this follows from equation 3.1). Moreover, critical points lying on this circle, being degenerate, have zero persistent strain rate σ and so cannot extend polymer chains. On figure 8*b*, plates 4 and 5, the only such degenerate critical point is the elliptic umbilic at $\omega = 0$ when the circle $R = \omega/2\gamma$ has shrunk to a point, but there is no reason in principle why fold and cusp points should not exist in polymer flows for some other sets of roller rates. Away from a degenerate critical point, σ increases, and so therefore does the birefringence (cf. figure 8(1*c*), plate 4). A theory of molecular extension in these circumstances will now be given.

Consider a critical point with extension index ν as defined by equations (3.3) or (3.4). The persistent strain rate is the strain rate along an outgoing streamline, that is

$$\sigma(r) = \frac{\mathrm{d}u}{\mathrm{d}r} = \nu k r^{\nu-1}. \tag{6.1}$$

Polymer chains in this flow will be considered as members of an ensemble of 'Hookean dumbbells' (Peterlin 1966) characterized by a relaxation time τ expressing the competition between fluid friction which tends to extend the chains and an elastic restoring force of entropic origin. With the high polymer concentrations employed in the six roll mill, entanglement of different chains is inevitable, and leads to non-Newtonian behaviour of the solution manifested by

Weissenberg effect (Weissenberg 1947) at the surface of the rollers. It is assumed that τ incorporates the effect of these entanglements. Molecular extension will be described by the r.m.s. value l of the component of the chain end-to-end vector lying along the streamline; by slight abuse of language $l(r)$ will be called the length of the chain at the point r. The unstretched length of the chains will be denoted by l_0; for N independent random links of length λ,

$$l_0 = \lambda\sqrt{(N/3)}. \tag{6.2}$$

The dumbbell model gives an equation for the time dependence of l in a flow with strain rate σ. In the present case σ is itself time dependent because macromolecules convect through the non-uniform flow field. Transforming the independent variable from time to r using $\mathrm{d}r/\mathrm{d}t = u(r)$ gives, as the equation for $l(r)$,

$$u(r)\frac{\mathrm{d}(l^2(r))}{\mathrm{d}r} + 2l^2(r)\left[\frac{1}{\tau} - \sigma(r)\right] = \frac{2l_0^2}{\tau}. \tag{6.3}$$

The solution corresponding to chains unextended at r_0 is easily verified to be

$$\frac{l^2(r)}{l^2(r_0)} = \frac{2u^2(r)}{\tau}\exp\left(-\frac{2}{\tau}\int_{r_0}^{r}\frac{\mathrm{d}r'}{u(r')}\right)\int_{r_0}^{r}\frac{\mathrm{d}r'}{u^3(r')}\exp\left(\frac{2}{\tau}\int_{r_0}^{r'}\frac{\mathrm{d}r''}{u(r'')}\right) + \frac{u^2(r)}{u^2(r_0)}\exp\left(-\frac{2}{\tau}\int_{r_0}^{r}\frac{\mathrm{d}r'}{u(r')}\right). \tag{6.4}$$

Only high extensions ($l \gg l_0$) are of interest in the present context, and it can be assumed that the chains are unextended at the critical point ($r_0 = 0$). In these limiting circumstances (6.4) gives, for a critical point with extension index ν,

$$l(r) = l_0 r^{\nu}\left[\frac{\tau k(\nu-1)}{2}\right]^{\nu/\nu-1}\sqrt{\left(\left(\frac{2}{\nu-1}\right)!\right)}. \tag{6.5}$$

This extension does not continue indefinitely. As l approaches the fully extended length $N\lambda$ strong non-Hookean forces act and the chain ceases to extend further or snaps. Full extension is reached at a distance r_H from the critical point given by

$$r_H = \frac{(3N)^{1/2\nu}}{\left[\frac{\tau k(\nu-1)}{2}\right]^{1/\nu-1}\left[\left(\left(\frac{2\nu}{\nu-1}\right)!\right)\right]^{1/2\nu}}. \tag{6.6}$$

Therefore the persistent strain rate σ_H at r_H satisfies

$$\sigma_H\tau = \frac{2\nu(3N)^{\nu-1/2\nu}}{(\nu-1)\left[\left(\left(\frac{2\nu}{\nu-1}\right)!\right)\right]^{\nu-1/2\nu}}. \tag{6.7}$$

As $\nu \to 1$ this expression tends to e^{-1} and merely reproduces the known result that near a hyperbolic critical point high extension occurs in strain rates exceeding a quantity of order τ^{-1}. As $\nu \to \infty$ (infinitely degenerate critical point), $\sigma_H\tau \to \sqrt{(6N)}$.

Obviously r_H is a measure of the size of the 'hole' of weak birefringence near the critical point. For the elliptic umbilic point $\nu = 2$ and $k = \gamma$ (equation 2.10), so that

$$r_H = (2N)^{\frac{1}{4}}/\tau\gamma. \tag{6.8}$$

In the six roll mill γ is known (equation 2.12) in terms of the roller speeds, so that a measure of the size of the birefringence hole can be used to give an estimate of τ even if N is very imprecisely known. When applied to figure 8(c1), assuming $N \approx 10^4$, this gives $\tau \approx 3$ s.

7. Conclusions

The central result of this work is the discovery of the qualitative difference in the six roll mill streamline patterns when the fluid does or does not contain polymer molecules. By contrast, streamlines in the flow between opposed jets (Mackey & Keller 1975) and in the four roll mill (Crowley *et al.* 1976) are unaffected by polymer, while in the two roll mill (Frank & Mackley 1976) the addition of polymer only causes the acute angle between streamlines issuing from a hyperbolic critical point to diminish without altering the topology of the streamlines. It is probable that the elliptic umbilic castastrophe describes the simplest family of flows in which the flow modification due to polymer causes topological changes in the streamlines.

There seems no reason to doubt that any polymer solution, in any concentration, would show effects similar to those reported here. For low concentrations the stream asymmetry $\alpha_+ - \alpha_-$ would be small, so that the rotated path in control space (1 2 3′ 4′ 5′ 6′ 7′ 8′ 9′ 10 on figure 3) would still intersect the catastrophe surface Σ twice. One of these intersections would, however, no longer lie on the cusp edge of Σ (8 on figure 3), so that the family of flows would show two fold catastrophes rather than one fold and one cusp. It was not possible to explore these flows with low concentration by using solutions of polyethylene oxide in water, because the flow became turbulent, even at low speeds, when the concentration was reduced below about 0.5 %.

It is tempting to regard the elliptic umbilic flow family as a rudimentary form of turbulence. in which a completely describable instability can give birth to a vortex (elliptic critical point) in several ways. Such an approach, which would consider in detail the origin and interactions of vortices – the 'atoms' of turbulence – would be complementary to the usual approaches based on the statistics of vorticity (Tennekas & Lumley 1972) or the instability of solutions of the Navier–Stokes equation (Ruelle & Takens 1971).

The six roll mill experiment does illustrate quite clearly that molecular extension of polymers occurs in these rather complex flows as thin sheets of oriented molecules within the flow. Moreover, it is possible that singular persistently extensional flows such as that in the six roll mill will feature in a full explanation of the Toms effect (Toms 1949). This is the reduction of turbulent drag by the addition of small amounts (of order 10^{-5}) of polymer, and has been plausibly supposed by Frank (1975) to be caused by localized persistent extension of the macromolecules.

However, such speculations relating the six roll mill to turbulence mechanisms should be regarded with a certain scepticism, because turbulence is time dependent and above all three-dimensional, whereas the flows considered in this paper are steady and essentially two-dimensional, being derived from a scalar stream function ϕ. The nonexistence of a stream function for general three-dimensional flows with vorticity means that elementary catastrophe theory cannot be employed to classify degenerate critical points. Non-degenerate critical points in an incompressible three-dimensional flow are the 'col' and 'col-foyer' in the classification of Poincaré (1886).

We thank Professor F. C. Frank, F.R.S., and Professor A. Keller, F.R.S., for many helpful discussions, Mr F. Bannister for supervising the construction of the mill, and Mr D. Read for photographic assistance. One of us (M.R.M) wishes to thank the Science Research Council for financial support.

PHILOSOPHICAL TRANSACTIONS OF THE ROYAL SOCIETY A MATHEMATICAL, PHYSICAL & ENGINEERING SCIENCES

References

Arnol'd, V. I. 1973 *Russ. Math. Survs.* (English translation from *Uspekhi Matematicheskikh Nauk*) **28**, 5, 19–48.
Crowley, D. G., Frank, F. C., Mackley, M. R. & Stephenson, R. G. 1976 *J. Polymer Sci.* **A2**, **14**, 1111–1119.
Frank, F. C. 1975 Invited Lecture at 50th Anniversary of the Canadian Pulp and Paper Institute, Montreal.
Frank, F. C. & Mackley, M. R. 1976 *J. Polymer Sci.* **A2**, **14**, 1121–1131.
Mackley, M. R. & Keller, A. 1975 *Phil. Trans. R. Soc. Lond.* **278**, 29–66.
Peterlin, A. 1966 *Pure appl. Chem.* **12**, 563–586.
Poincaré, H. 1886 *J. Math.* **4**, 2, 151–217.
Ruelle, D. & Takens, F. 1971 *Comm. math. Phys.* **20**, 167–192.
Tennekes, H. & Lumley, J. L. 1972 *A first course in turbulence.* Cambridge, Mass: M.I.T. Press.
Thom, R. 1972 *Stabilité structurelle et morphogénèse.* Reading, Mass: Benjamin (English trans. (1975) *Structural stability and morphogenesis*).
Toms, B. A. 1949 *Proc. First Int. Congr. Rheology* (Scheveningen) 135–141.
Weissenberg, K. 1947 *Nature* **159**, 310–311.

PHILOSOPHICAL TRANSACTIONS OF THE ROYAL SOCIETY A MATHEMATICAL, PHYSICAL & ENGINEERING SCIENCES

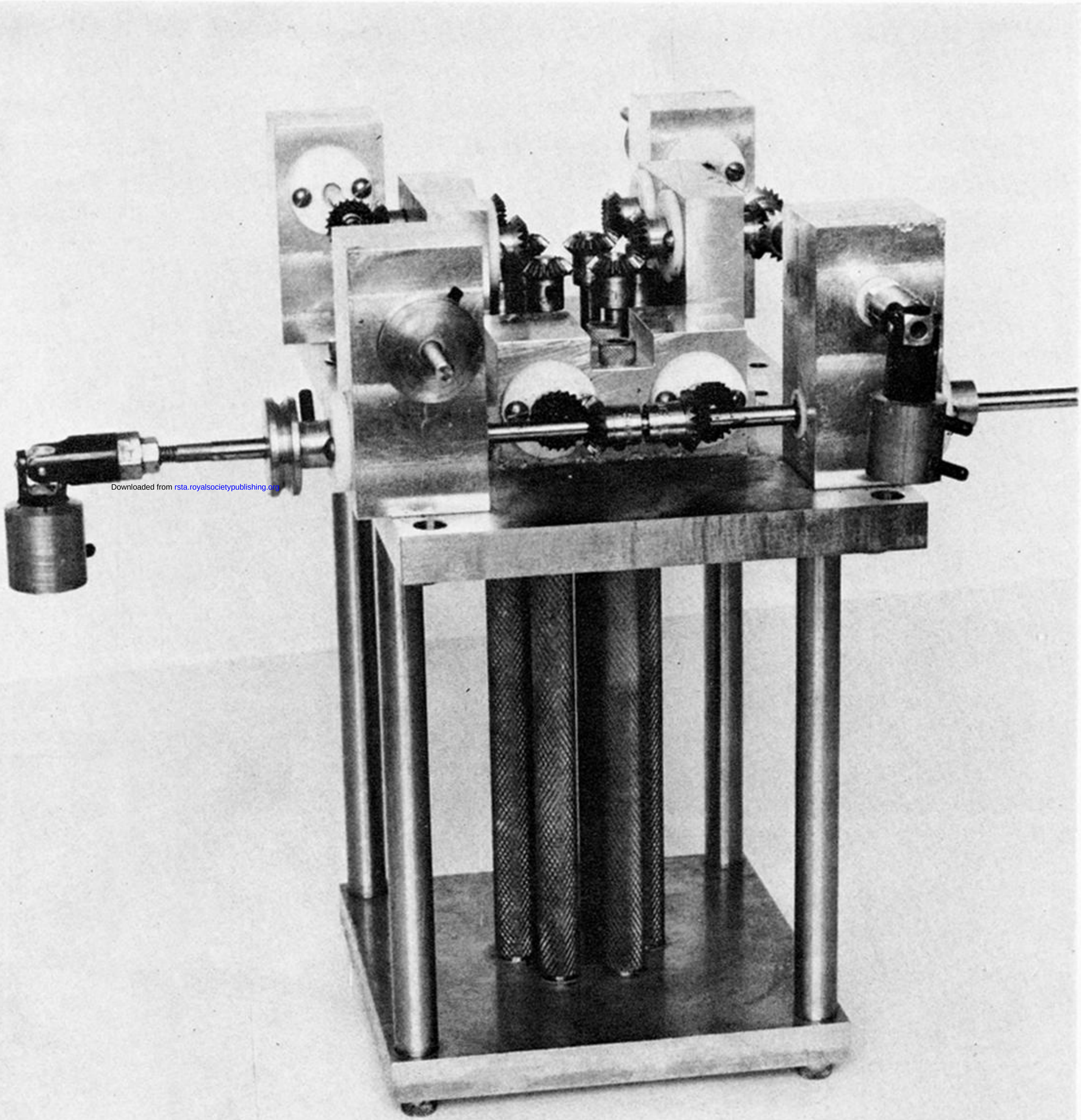

FIGURE 6. Photograph of six roll mill.

PHILOSOPHICAL TRANSACTIONS OF THE ROYAL SOCIETY A MATHEMATICAL, PHYSICAL & ENGINEERING SCIENCES

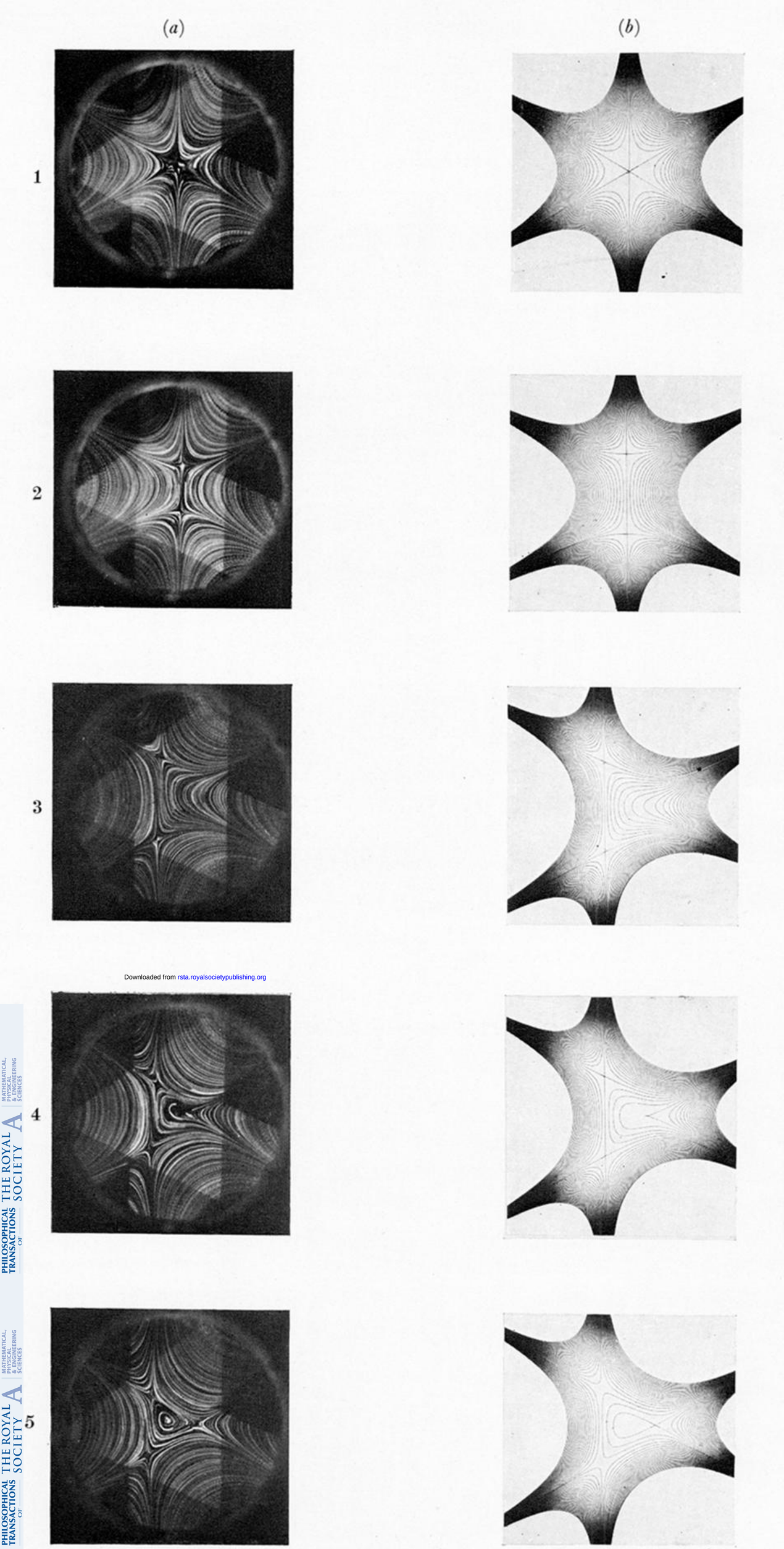

FIGURE 7. For description see opposite.

PHILOSOPHICAL TRANSACTIONS OF THE ROYAL SOCIETY A MATHEMATICAL, PHYSICAL & ENGINEERING SCIENCES

(*a*) (*b*)

6 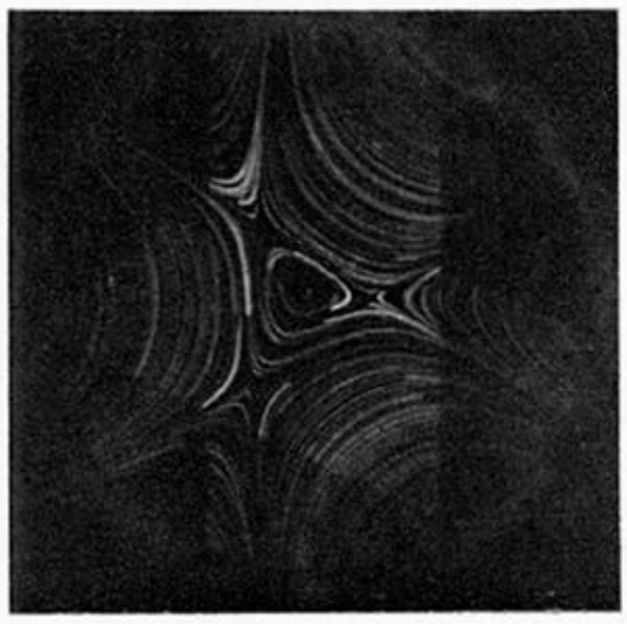

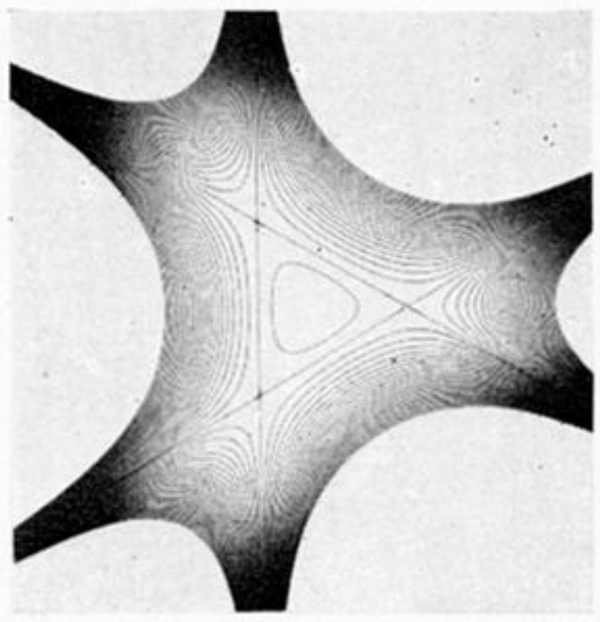

7 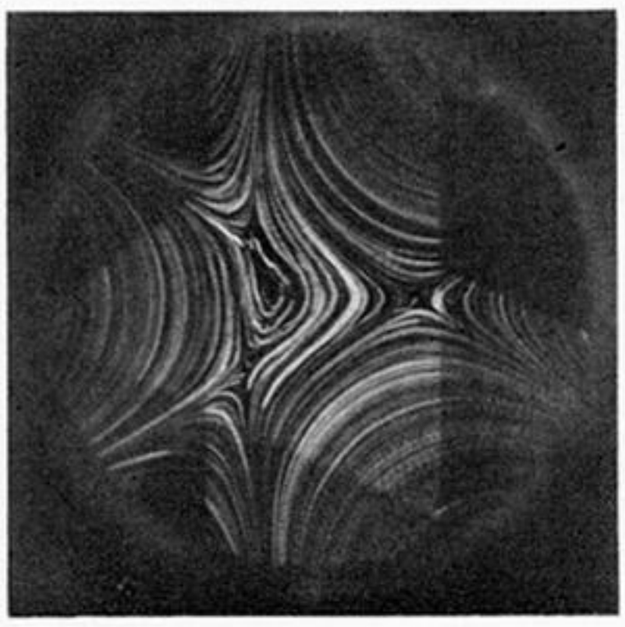

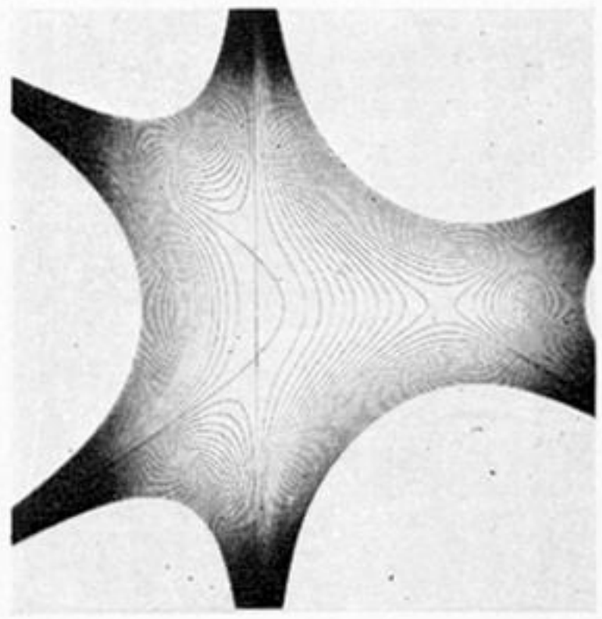

8 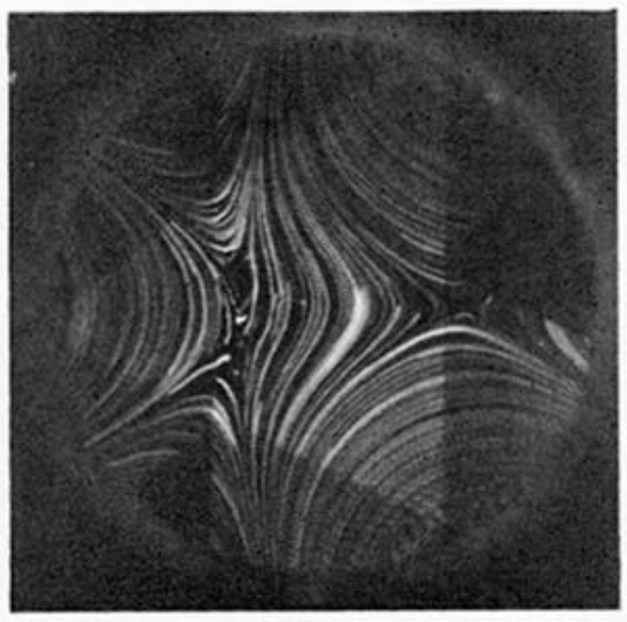

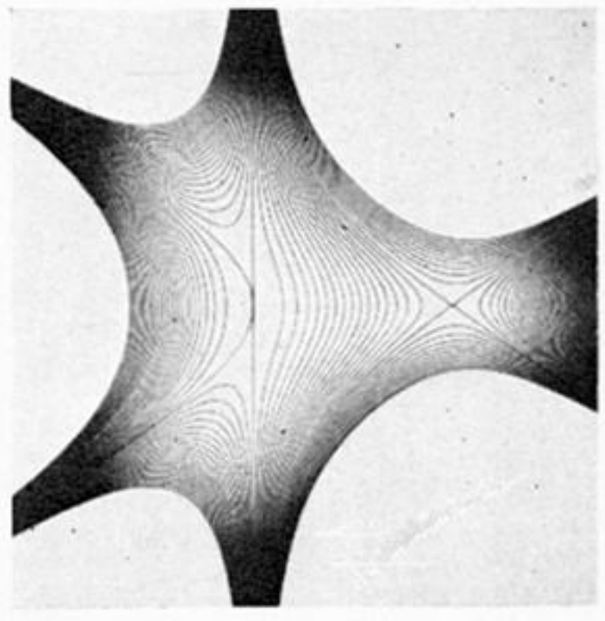

9 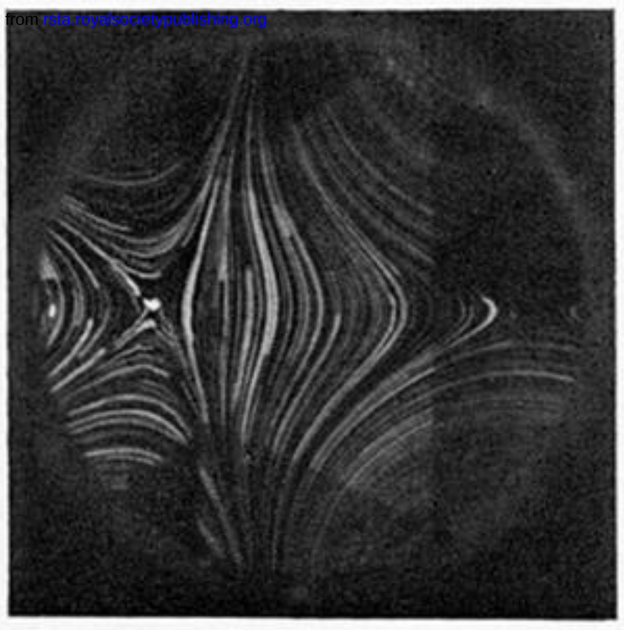

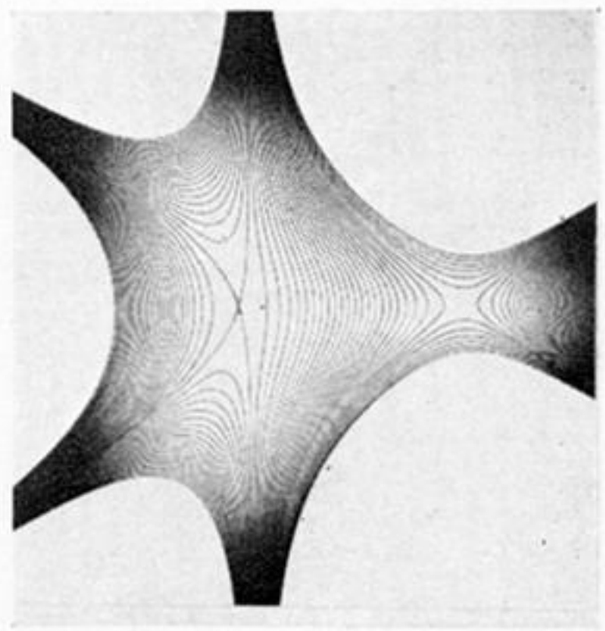

10 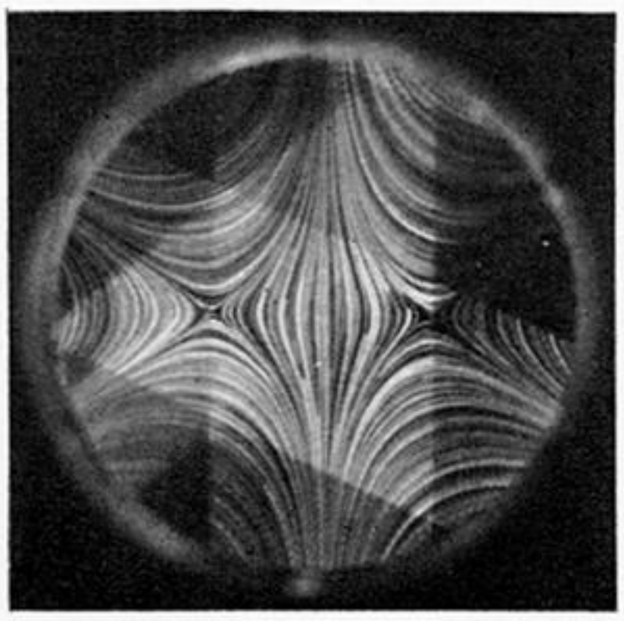

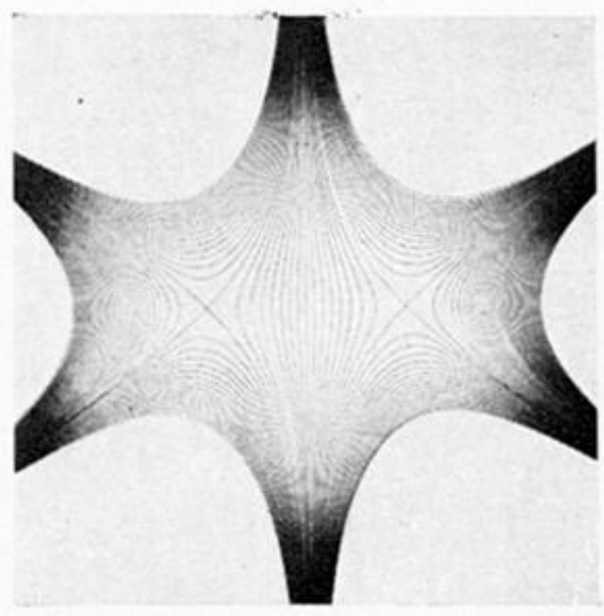

FIGURE 7. (*a*) Flows 1 to 10 of glycerol in the six roll mill, corresponding to roller speeds Ω_{I}, Ω_{II} and Ω_{III} of table 1. (*b*) Computer simulations of flows 1 to 10 with control parameters ω/γ and V_y/γ of table 1.

(a) (b) (c)

1

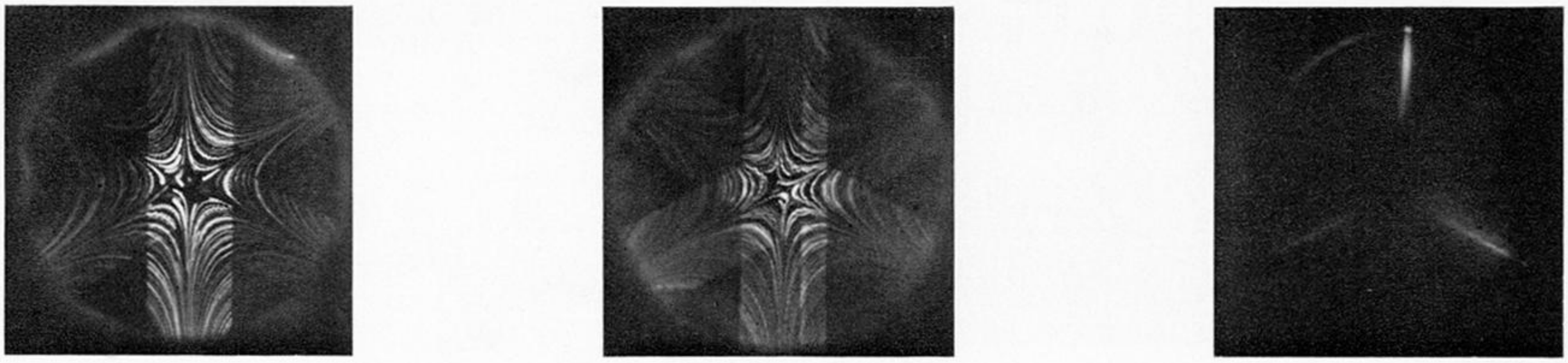

2

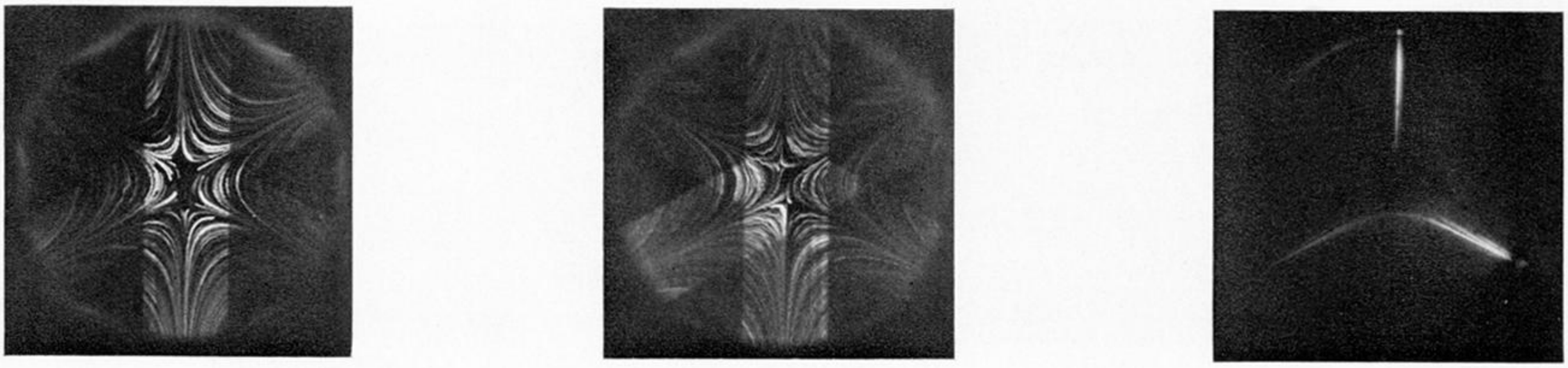

3

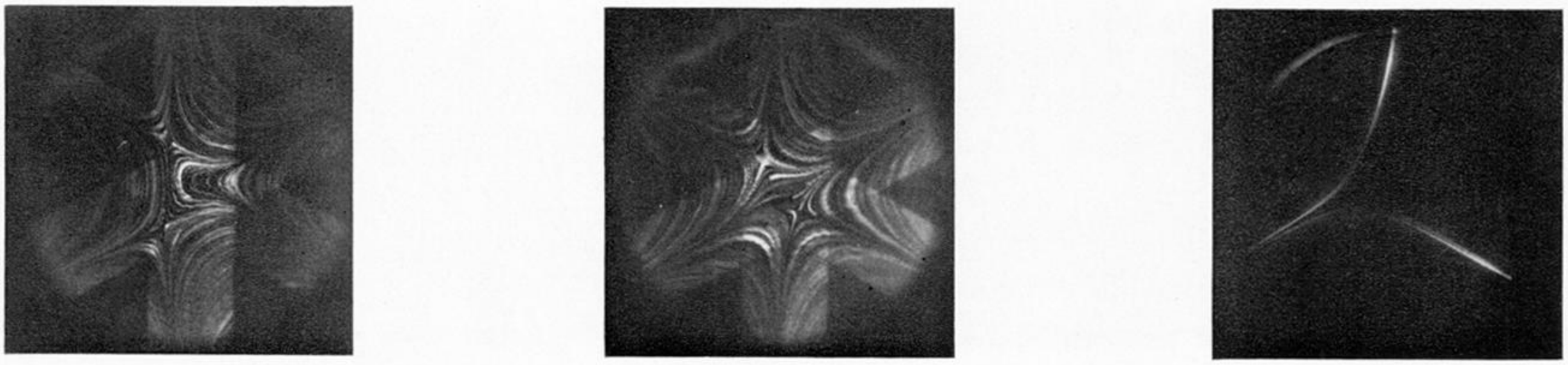

4

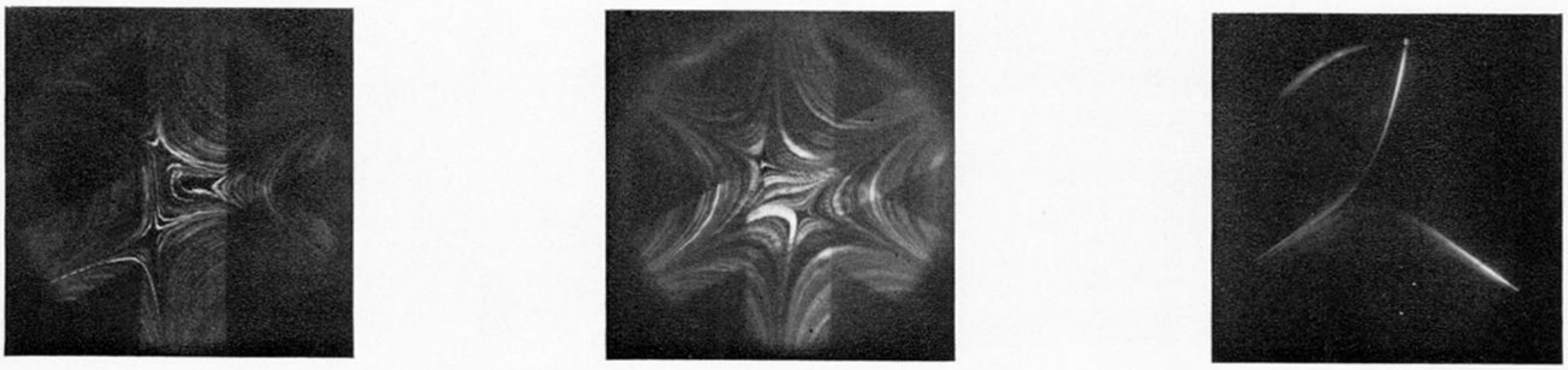

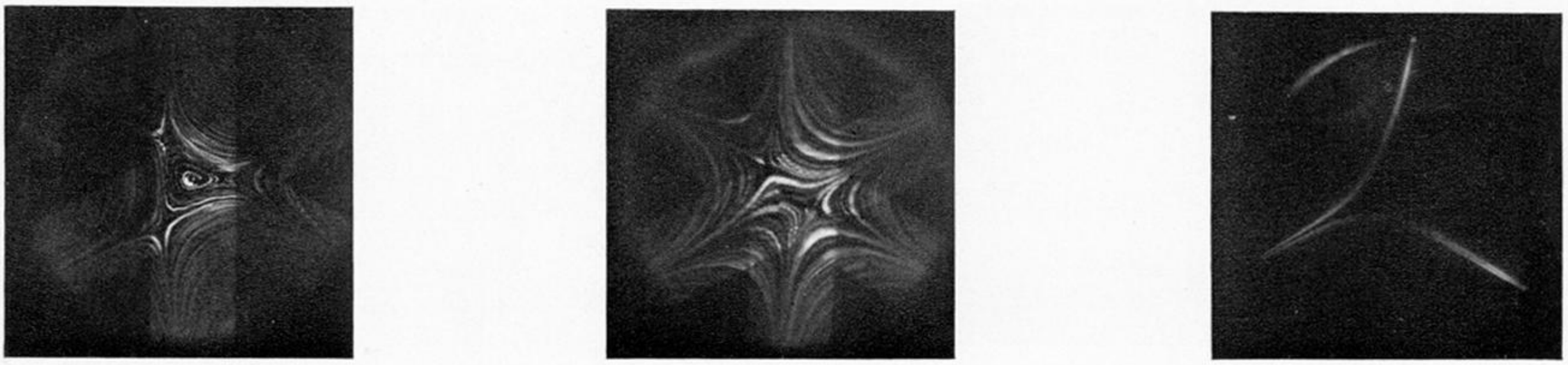

FIGURE 8. For description see opposite.

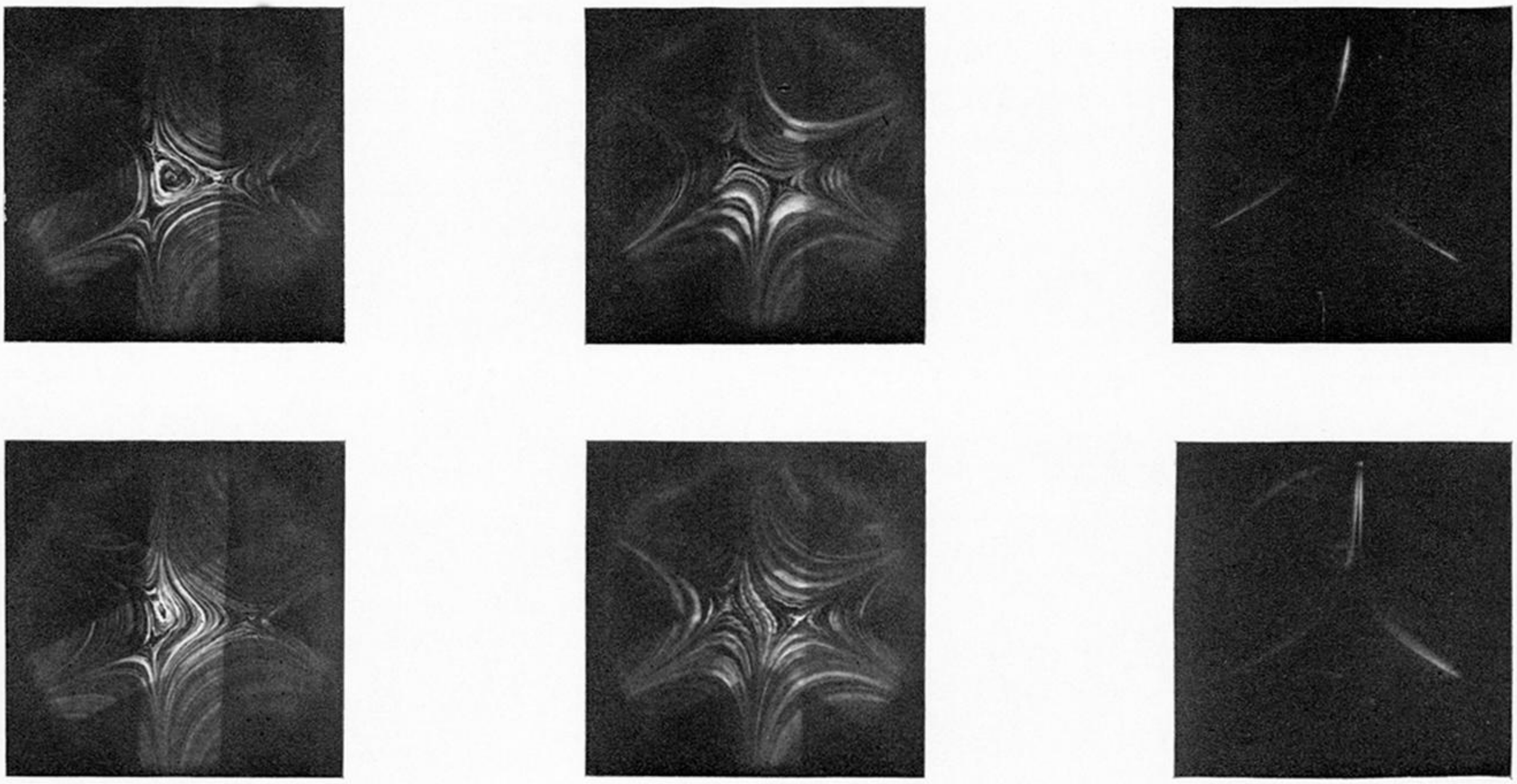

FIGURE 8. Streamline patterns of (*a*) glycerol and (*b*) 2% polyethylene oxide solution in the six roll mill corresponding to roller speeds Ω_{I}, Ω_{II} and Ω_{III} of table 2. (*c*) Corresponding flow birefringence observations of the polyethylene oxide solution.